

Reduction of Strained Polycycles: How Much Strain Can a Pyrene Anion Take?

Ivan Aprahamian,[†] Graham J. Bodwell,[‡] Jim J. Fleming,[‡] Greg P. Manning,[‡] Michael R. Mannion,[‡] Brad L. Merner,[‡] Tuvia Sheradsky,[†] Rudolf J. Vermeij,[‡] and Mordecai Rabinovitz^{*†}

Contribution from the Department of Organic Chemistry, The Hebrew University of Jerusalem, Jerusalem 91904, Israel, and Department of Chemistry, Memorial University of Newfoundland, St. John's, NL, Canada A1B 3X7

Received February 3, 2004; E-mail: mordecai@vms.huji.ac.il

Abstract: The reduction of a series of $[n](2,7)$ pyrenophanes ($n = 7-10$) with lithium or potassium metal shows that the strain in the system, controlled by the length of the tether, determines the nature of the reduction products. The reduction of $[7](2,7)$ pyrenophane (**2**) and $[2]$ metacyclo $[2](2,7)$ pyrenophane (**3**) leads to reductive dimerization followed by novel intramolecular σ -bond formation as a means of escaping strained anti-aromaticity. $[8](2,7)$ Pyrenophane (**4**) affords only reductive dimerization, and no two-electron reduction is observed. The reduction of $[9](2,7)$ pyrenophane (**5**) and $[10](2,7)$ pyrenophane (**6**) leads to reductive dimerization, followed by the formation of a dianionic anti-aromatic species, which eventually cleaves the solvent, THF- d_6 . The similarity between the reduction of the latter systems and the reduction of pyrene (**1**) is discussed.

Introduction

The discovery of fullerenes¹ and the subsequent isolation of C_{60} ² have rekindled interest in the study of curved polycyclic aromatic hydrocarbons (PAHs), especially those that can be mapped onto the surface of C_{60} or other fullerenes.³ A well-studied aspect of such curved systems is their aromatic behavior,⁴ as such systems can help to clarify the nature of aromaticity as they manifest a compromise between strain and conjugation.^{3d,5}

The effect of curvature on the aromatic character of PAHs can be studied by comparing planar PAHs and their curved analogues. Recently a variety of $[n](2,7)$ pyrenophanes in which pyrene (**1**) is strongly distorted from planarity have been

synthesized and studied in order to address this issue.⁶ The degree of distortion from planarity and therefore the strain in these systems can be controlled by the length and type of the tether that connects the two remote ends (positions 2 and 7) of **1**; the shorter the tether, the greater the strain. It was found that it is possible to bend the pyrene unit, which is found in the surfaces of several fullerenes and buckybowls of such systems to a greater extent than that of the pyrene unit in C_{70} .^{6b} The studies also showed that enforcing nonplanarity in the pyrene nucleus does little to diminish the anisotropy effect of the bent systems. This means that, despite the enforced curvature, the pyrene system still maintains most of its aromatic character.

The aromaticity of **1** can be rationalized by the "peripheral model",⁷ since it has $4n + 2$ conjugated π -electrons at the periphery. This model emphasizes the contribution of peripheral π -conjugation to the aromatic character of the system and considers the inner bonds to be a bridging perturbation to the annulene skeleton. It is possible to convert **1** into an anti-aromatic entity by adding two electrons to its periphery. This can be achieved by alkali metal reduction.⁸

[†] The Hebrew University of Jerusalem.

[‡] Memorial University of Newfoundland.

(1) Kroto, H. W.; Heath, J. R.; O'Brien, S. C.; Curl, R. F.; Smalley, R. E. *Nature* **1985**, *318*, 162.

(2) Krätschmer W.; Lamb L. D.; Fostiropoulos, K.; Huffman, D. R. *Nature* **1990**, *347*, 354.

(3) For recent reviews on bowl-shaped, fullerene-related hydrocarbons, see: (a) Siegel, J. S.; Seiders, T. J. *Chem. Ber.* **1995**, *313*. (b) Faust, R. *Angew. Chem., Int. Ed. Engl.* **1995**, *34*, 1429. (c) Rabideau, P. W.; Sygula, A. In *Advances in Theoretically Interesting Molecules*; Thummel, R. P., Ed.; JAI Press: Greenwich, CT, 1995; Vol. 3, p 1. (d) Rabideau, P. W.; Sygula, A. *Acc. Chem. Res.* **1996**, *29*, 235. (e) Scott, L. T. *Pure Appl. Chem.* **1996**, *68*, 291. (f) Mehta, G.; Rao, H. S. P. Tetrahedron Report Number 470. *Tetrahedron* **1998**, *54*, 13325.

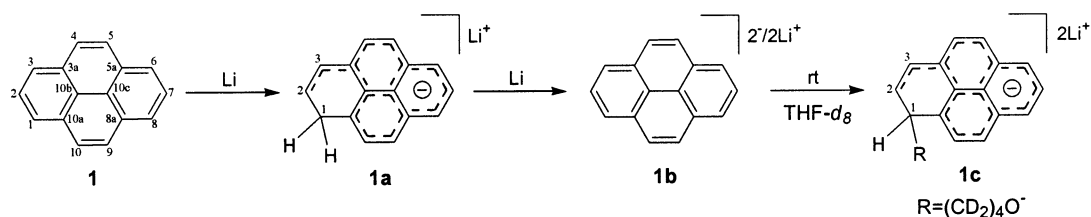
(4) For example, see: (a) Ferrer, S. M.; Molina, J. M. J. *Comput. Chem.* **1999**, *20*, 1412. (b) Steiner, E.; Fowler, P. W.; Jenneskens, L. W. *Angew. Chem., Int. Ed.* **2001**, *40*, 362. (c) Poater, J.; Frader, X.; Duran, M.; Solà, M. *Chem.—Eur. J.* **2003**, *9*, 1113.

(5) For some recent reviews about aromaticity and its structural aspects, see: (a) Schleyer, P. v. R.; Jiao, H. *Pure Appl. Chem.* **1996**, *68*, 209. (b) Krygowski, T. M.; Cyrański, M. K.; Czarnocki, Z.; Häfelinger, G.; Katritzky, A. R. Tetrahedron Report Number 520. *Tetrahedron* **2000**, *56*, 1783. (c) Krygowski, T. M.; Cyrański, M. K. *Chem. Rev.* **2001**, *101*, 1385.

(6) (a) Bodwell, G. J.; Bridson, J. N.; Houghton, T. J.; Kennedy, J. W. J.; Mannion, M. R. *Angew. Chem., Int. Ed.* **1996**, *35*, 1320. (b) Bodwell, G. J.; Bridson, J. N.; Houghton, T. J.; Kennedy, J. W. J.; Mannion, M. R. *Chem.—Eur. J.* **1999**, *5*, 1823. (c) Bodwell, G. J.; Fleming, J. J.; Mannion, M. R.; Miller, D. O. *J. Org. Chem.* **2000**, *65*, 5360. (d) Bodwell, G. J.; Bridson, J. N.; Cyrański, M. K.; Kennedy, J. W. J.; Krygowski, T. M.; Mannion, M. R.; Miller, D. O. *J. Org. Chem.* **2003**, *68*, 2089.

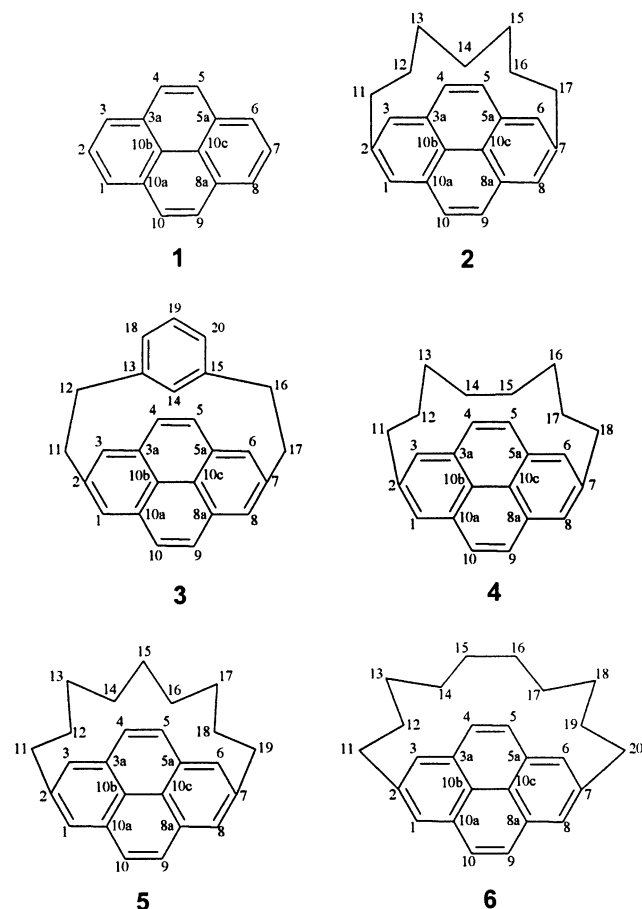
(7) (a) Dewar, M. J. S. *J. Am. Chem. Soc.* **1952**, *74*, 3341. (b) Platt, J. R. *J. Chem. Phys.* **1954**, *22*, 1448.

(8) (a) Müllen, K. *Helv. Chim. Acta* **1978**, *61*, 2307. (b) Minsky, A.; Meyer, A. Y.; Rabinovitz, M. *J. Am. Chem. Soc.* **1982**, *104*, 2475. (c) Schnieders, C.; Müllen, K.; Huber, W. *Tetrahedron* **1984**, *40*, 1701. (d) Eliasson, B.; Lejon, T.; Edlund, U. *J. Chem. Soc., Chem. Commun.* **1984**, 591.

Scheme 1. Reduction Process of **1** with Lithium Metal

The reduction of PAHs with alkali metals⁹ yields negatively charged π -conjugated molecules that may undergo structural changes from structural distortions,¹⁰ rearrangements,¹¹ and aggregations¹² to the formation of new chemical bonds,¹³ as is the case in reductive dimerization processes.¹⁴ The reduction of **1** can yield different products, depending on solvent, counterion, and temperature. Three successive diamagnetic species can be detected when **1** is reduced with lithium metal in THF-*d*₈ (Scheme 1): a protonated pyrene monoanion (**1a**), a dianion (**1b**), and finally a monoanion that incorporates the atoms of a former solvent molecule (solvent cleavage) (**1c**).^{8c} Recently we have shown¹⁵ that the reduction of the two strained pyrene systems, [7](2,7)pyrenophane (**2**)^{6c} and [2]metacyclo[2](2,7)pyrenophane (**3**),¹⁶ with lithium metal affords totally different results than those encountered in the reduction of the planar parent pyrene system.¹⁷ The reduction of these systems shows that the strain in the pyrene moiety profoundly affects its reactivity.

The pyrene (**1**), [n](2,7)pyrenophane (*n* = 7–10; **2**, **4**, **5** and **6**) and [2]metacyclo[2](2,7)pyrenophane (**3**) molecules



Here we report a comprehensive systematic study of the reduction of a series of pyrene-based strained molecules. The

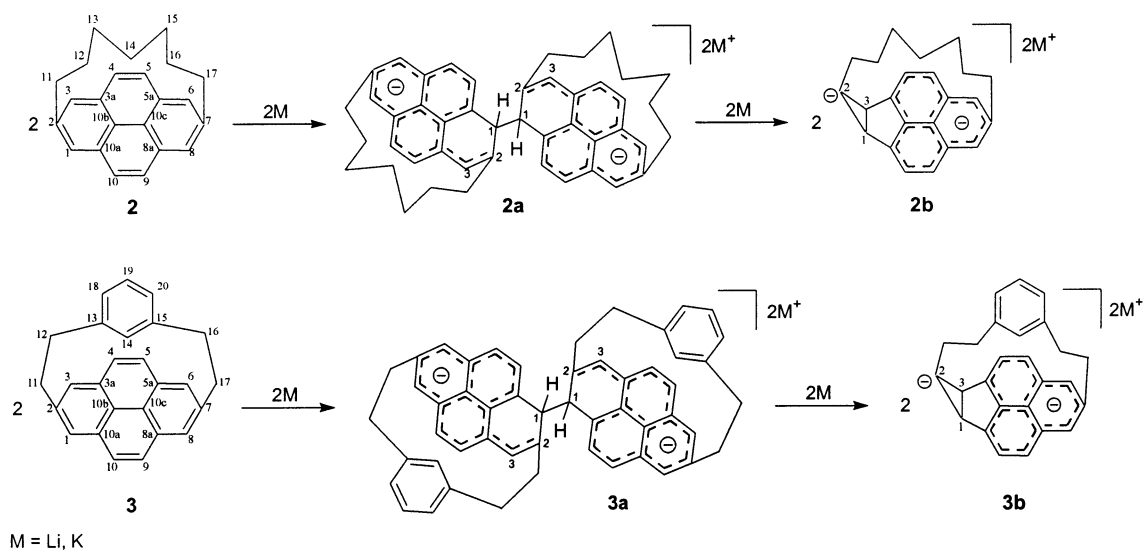
study was conducted to understand the effect strain can have on the reduction process of **1** and assess whether a limit exists to the degree of curvature **1** can withstand, without undergoing skeletal changes. The investigation was carried out by reducing a series of [n](2,7)pyrenophanes (*n* = 7–10), in which the degree of distortion from planarity of the pyrene unit varies with tether length,^{6c} with alkali metals. The characterization of the resulting anionic species (structure and aromatic behavior) was achieved using various NMR spectroscopy methods.

Results and Discussion

Tether of Seven Carbon Atoms: [7](2,7)Pyrenophane (**2**) and [2]metacyclo[2](2,7) pyrenophane (**3**) that have tethers of seven carbons have been reduced with lithium¹⁵ and potassium metals (Scheme 2). The reduction process was monitored by NMR spectroscopy. Both **2** and **3** show similar two-step reduction processes, which means that the isolated benzene ring in **3** has a negligible effect on the overall reduction process. This also indicates that the electron transfer through the “cyclophane hub”¹⁸ is minimal. In both cases the reduction is accompanied by symmetry changes that are observable in the ¹H NMR and ¹³C NMR spectra.¹⁹

A. One-Electron Reduction.^{15b} The reduction of **2** (colorless) and **3** (yellow) with lithium or potassium metal (Scheme 2) gives the dimeric diamagnetic species **2a** (wine-red) and **3a** (brown) that show no dynamic processes in their ¹H NMR spectra over a wide range of temperatures (165–273 K). The dimers were identified by the high field absorption of carbon atom **C1** in species **2a** and **3a** (δ = 48.3 and 48.7 ppm, respectively, Table 1) and the magnitude of its ¹J_{C,H} coupling (128.2 and 130.0 Hz for **2a** and **3a**, respectively, Table 1), which are compatible with

- (9) For a review about the alkali metal reduction of PAHs, see: Benschaftr, R.; Shabtai, E.; Rabinovitz, M.; Scott, L. T. *Eur. J. Org. Chem.* **2000**, 1091.
- (10) For example: Eshdat, L.; Ayalon, A.; Beust, R.; Shenhar, R.; Rabinovitz, M. *J. Am. Chem. Soc.* **2000**, *122*, 12637.
- (11) For example, see: Eshdat, L.; Berger, H.; Hopf, H.; Rabinovitz, M. *J. Am. Chem. Soc.* **2002**, *124*, 3822.
- (12) (a) Ayalon, A.; Sygula, A.; Cheng, P.-C.; Rabinovitz, M.; Rabideau, P. W.; Scott, L. T. *Science* **1994**, *265*, 1065. (b) Shenhar, R.; Wang, H.; Hoffman, R. E.; Frish, L.; Avram, L.; Willner, I.; Rajca, A.; Rabinovitz, M. *J. Am. Chem. Soc.* **2002**, *124*, 4685.
- (13) For example, see: Bock, H.; Havlas, Z.; Gharagozloo-Hubmann, K.; Sievert, M. *Angew. Chem., Int. Ed.* **1999**, *38*, 2240.
- (14) (a) Bergmann, E. D. *Chem. Rev.* **1968**, *68*, 41. (b) Edlund, U.; Eliasson, B. J. *Chem. Soc., Chem. Commun.* **1982**, 950. (c) Baumgarten, M.; Müllen, K. *Top. Curr. Chem.* **1994**, *169*, 1. (d) Aprahamian, I.; Hoffman, R. E.; Sheradsky, T.; Preda, D. V.; Bancu, M.; Scott, L. T.; Rabinovitz, M. *Angew. Chem., Int. Ed.* **2002**, *10*, 1712.
- (15) (a) Aprahamian, I.; Bodwell, G. J.; Fleming, J. J.; Manning, G. P.; Mannion, M. R.; Sheradsky, T.; Vermeij, R. J.; Rabinovitz, M. *J. Am. Chem. Soc.* **2003**, *125*, 1720. (b) Aprahamian, I.; Bodwell, G. J.; Fleming, J. J.; Manning, G. P.; Mannion, M. R.; Sheradsky, T.; Vermeij, R. J.; Rabinovitz, M. *Angew. Chem., Int. Ed.* **2003**, *42*, 2547.
- (16) Bodwell, G. J.; Miller, D. O.; Aprahamian, I.; Rabinovitz, M.; Sheradsky, T.; Vermeij, R. J. In preparation.
- (17) Pyrene was also reduced, under our conditions, for comparison.
- (18) (a) Gerson, F.; Martin, W. B., Jr.; Wylder, C. *Helv. Chim. Acta* **1976**, *59*, 1365. (b) Shabtai, E.; Rabinovitz, M.; König, B.; Knieriem, B.; de Meijere, A. *J. Chem. Soc., Perkin Trans. 2* **1996**, 2589.

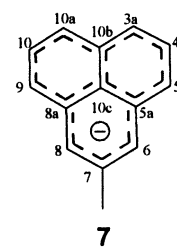
Scheme 2. Reduction Process of **2** and **3** with Lithium or Potassium Metal**Table 1.** ^{13}C NMR and ^1H NMR (in Parentheses) Chemical Shifts, in ppm, of the Pyrene Moiety of the Lithium Salt of **2a**, **2b**, **3a**, and **3b** in $\text{THF}-d_6^a$

	C1 (H1)	C2	C3 (H3)	C3a	C4 (H4)	C5 (H5)	C5a	C6 (H6)	C7	C8 (H8)	C8a	C9 (H9)	C10 (H10)	C10a	C10b	C10c
2a	48.3 ^b (3.2)	99.4	129.6 (5.8)	110.6	131.9 (6.6)	102.7 (5.7)	142.2	119.3 (5.6)	135.5	114.8 (5.7)	142.7	110.0 (5.9)	129.7 (6.0)	105.2	140.6	135.8
2b	33.9 (2.3)	29.2	33.9 (2.3)	118.5	125.7 (6.2)	101.6 (5.2)	145.8	107.9 (5.1)	141.6	107.9 (5.1)	145.8	101.6 (5.2)	125.7(6.2)	118.5	147.6	136.9
3a	48.7 ^c (3.4)	95.7	129.0 (5.9)	113.1	129.8 (6.3)	102.6 (5.3)	142.4	118.3 (5.2)	131.7	114.1 (5.8)	143.0	109.3 (6.0)	129.1 (5.9)	103.5	140.5	135.8
3b	33.7 (2.4)	30.1	33.7 (2.4)	118.1	125.6 (6.2)	101.6 (5.1)	145.1	108.1 (4.8)	140.5	108.1 (4.8)	145.1	101.6 (5.1)	125.6 (6.2)	118.1	146.9	136.5
7^d				103.1	128.1	103.1	144.5	104.3	135.2	104.3	144.7	103.1	128.1	103.1	144.7	137.6

^a The ^{13}C NMR chemical shifts of **7** are also added for comparison. ^b $^1J_{\text{C1,H1}} = 128.2$ Hz, $^3J_{\text{H1,*H1}} = 10.3$ Hz. ^c $^1J_{\text{C1,H1}} = 130.0$ Hz, $^3J_{\text{H1,*H1}} = 10.6$ Hz. ^d Taken from ref 21.

sp^3 -hybridization. In addition, an indication that a new σ -bond has been formed between two identical **C1** carbons comes from the heteronuclear multiple-bond correlation (HMBC) experiment, which shows a correlation between carbon atom **C1** and hydrogen atom **H1**. The $^3J_{\text{H1,*H1}}$ couplings (derived from the proton-coupled heteronuclear single quantum coherence sensitivity-improved (HSQCSI) experiments)²⁰ were measured to be 10.3 and 10.6 Hz for **2a** and **3a** (Table 1), respectively, which is appropriate for dimers with an anti conformation about the new σ -bond.

The dimerization of **2** and **3** can be explained by means of a radical coupling at carbon atom **C1**. Such radical coupling will leave a negative charge on carbon atom **C2** that can be delocalized over the carbon atoms on the periphery of a phenalene subunit, which explains why two sets of carbon atoms are observed in the ^{13}C NMR spectra (one at $\delta = 99$ –119 and the other at $\delta = 129$ –143 ppm). The good agreement between the carbon chemical shifts of the phenalene moiety of **2a** and **3a** and those of the 2-methylphenalenyl anion (**7**)²¹ clearly supports this conclusion (Table 1).

The 2-methylphenalenyl anion (**7**)

B. Two-Electron Reduction.^{15a} In the second reduction process, the “intermolecular” σ -bond between the two carbon **C1** atoms of the dimer is cleaved, to afford the monomers **2b** (wine-red) and **3b** (brown). **2a** and **3b** have a new *intramolecular* σ -bond that transforms one of the benzene rings into a “cyclopropano–cyclopentano” (bicyclo[3.1.0]) ring system.²² The new σ -bond explains the high field absorption of carbon atom **C1** (33.9 and 33.7 ppm for **2a** and **3a**, respectively, Table 1) and its one-bond CH-coupling ($^1J_{\text{C1,H1}} = 163.2$ and 162.3 Hz for **2b** and **3b**, respectively). These values are consistent with a strained sp^3 -hybridized carbon, as is the case in a cyclopropane ring.²³ The $^3J_{\text{H1,*H1}}$ coupling constant (9.1 and 8.7

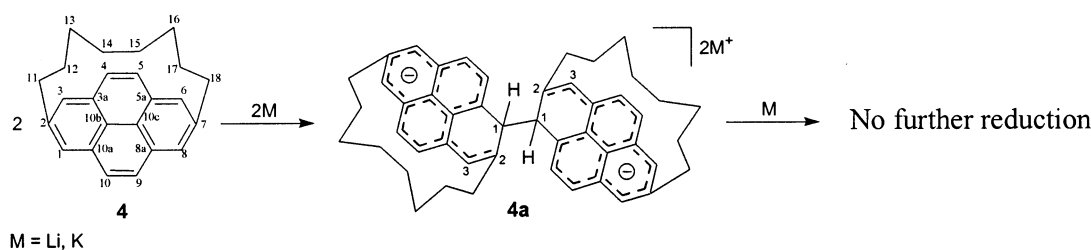
(19) For the sake of clarity, the results of the lithium reduction will be discussed for all the molecules. Any dissimilarity, should it exist, between the lithium and potassium reductions will be noted.

(20) (a) Palmer, A. G., III; Cavanagh, J.; Wrights, P. E.; Rance, M. *J. Magn. Reson.* **1991**, *93*, 151. (b) Kay, L. E.; Keifer, P.; Saarinen, T. *J. Am. Chem. Soc.* **1992**, *114*, 10663.

(21) Hopenius, M. A.; Heinen, W.; Mulder, P. P. J.; Erkelens, C.; Zuilhof, H.; Lugtenburg, J.; Cornelisse, J. *J. Phys. Org. Chem.* **1994**, *7*, 296.

(22) A dynamic process is observed in the ^1H NMR of **2b** and **3b**, which in some cases further lowers the symmetry of the system. For the sake of clarity, the chemical shifts of the systems with higher symmetry are discussed.

(23) Günther, H. *NMR Spectroscopy – An Introduction*; Wiley: Chichester, U.K., 1980.

Scheme 3. Reduction Process of **4** with Lithium or Potassium Metal

Hz for **2b** and **3b**, respectively) and the correlation seen in the HMBC experiments between hydrogen atom **H1** and carbon atom **C2** are also explained by the formation of this new σ -bond. In this scenario the high-field shift of carbon atom **C2** (29.2 and 30.1 ppm for **2b** and **3b**, respectively) results from the localization of the charge on it.

It can be seen in **2b** and **3b** that the phenalenyl anion is still intact. This is evident from the high-field shift of carbon atoms **C8**, **C9**, and **C10a** (and their symmetrically equivalent atoms) and hydrogen atoms **H8** and **H9**, which constitute a section of the periphery of phenalene (Table 1).

As far as the tether is concerned, the most interesting result comes from following after the chemical shift of hydrogen atom **H14** in compound **3**, and its reduction products, **3a** and **3b**. In neutral **3** this phenyl hydrogen absorbs at $\delta = 4.10$ ppm, as a result of a strong anisotropy effect.¹⁶ In **3a** the absorption is at $\delta = 5.10$ ppm, indicating the presence of diamagnetic ring currents in the “phenalenyl anion” (what remains of the pyrene moiety). To the best of our knowledge, this is the first time that the anisotropy effect above the core of a phenalenyl anion has been measured experimentally. The phenalenyl anion is still intact in **3b**, but hydrogen atom **H14** absorbs at a lower field ($\delta = 6.83$ ppm), characteristic of aromatic hydrogens. This may be due to one or a combination of two reasons: (1) the cyclopropyl ring moves the benzene ring away from the core of the phenalenyl anion, and thus **H14** is less affected by the anisotropy effect; 2) The dynamics of the tether cancels the effect.

C. Dynamic NMR. ¹H NMR spectra were recorded for **2b** and **3b** at various temperatures in order to follow the dynamic process of the tether, which affects the axis of symmetry along it and to estimate its free energy of activation. The ΔG^\ddagger values were calculated from the coalescence temperatures using the Eyring equation.²³

Lowering the temperature in **2b** does not result in line splitting but rather in broadening, which hinders the calculation of ΔG^\ddagger .²⁴ In **3b**, the signal of hydrogen atom **H9**, which appears as a doublet at 260 K ($\delta = 5.11$ ppm), broadens at lower temperatures and is finally split into two broad doublets at 165 K ($\delta = 5.85$ and 4.82 ppm).²⁵ The ΔG^\ddagger of this process is calculated to be 9.1 ± 0.2 kcal/mol.

D. Quench Experiments. Oxygen-quench experiments conducted on **2a** and **3a** afforded the neutral species **2** and **3**. This indicates that the carbon framework of the original polycyclic moiety did not degrade as a result of reduction. In contrast, an

oxygen quench of **3b** gave an irresolvable NMR spectrum. Attempts to quench the dianion **3b** were also made with iodine and dimethyl sulfate, and in both cases the product readily underwent polymerization.

Tether of Eight Methylene Carbons: [8](2,7)Pyrenophane (**4**)^{6c} was reduced with lithium and potassium metals. The reduction is accompanied by color change from a colorless to wine-red solution. Only one reduction product was observed in both cases (Scheme 3). The NMR data show that **4** also undergoes a reductive dimerization to produce a dianionic dimer, **4a**. Prolonged contact with either lithium or potassium metals did not reduce the dimer any further. Oxygen quench experiments conducted on **4a** afforded neutral **4**.

Tether of Nine Methylene Carbons: [9](2,7)Pyrenophane (**5**)^{6c} (colorless) was reduced with lithium and potassium metals to afford a paramagnetic species followed by three different diamagnetic reduction products (Scheme 4); here as well, the reduction was observable via the color change of the solution.¹⁹

A. One-Electron Reduction. The first reduction product of **5** is probably a radical anion (orange solution), since it does not show a ¹H NMR spectrum. The paramagnetic species is followed by a dianionic dimer, **5a** (wine-red), which is afforded via radical coupling. It is worth noting that this dimer is less soluble than the previous ones. Quench of **5a** with oxygen gave the neutral species **5**.

B. Two-Electron Reduction. Upon further reduction, the ¹H NMR spectrum of the dimer disappears and a flat spectrum is obtained. When the ¹H NMR spectrum is measured at temperatures below 200 K, a new set of broad peaks appears. This means that the new species is in singlet–triplet equilibrium, with a higher contribution of the triplet state and, thus, can only be observed at low temperatures. The ¹H and ¹³C NMR spectra of the new species **5b** (brown-red when reduced with lithium and blue with potassium) are relatively less complex than those of the dimer. The broadness of the peaks is a result of both the singlet–triplet equilibrium and the tether dynamics (to be discussed). It can be seen that **5b** has only two proton absorptions belonging to the pyrene entity: $\delta = 1.44$ and 2.58 ppm for hydrogen atoms **H1** and **H10**, respectively.²⁶ It is evident from the high-field shift of these ¹H NMR absorptions that the second reduction product is an anti-aromatic species (**5b**). This explains the presence of the singlet–triplet equilibrium in **5b**, for it is characteristic of anti-aromatic systems.²⁷

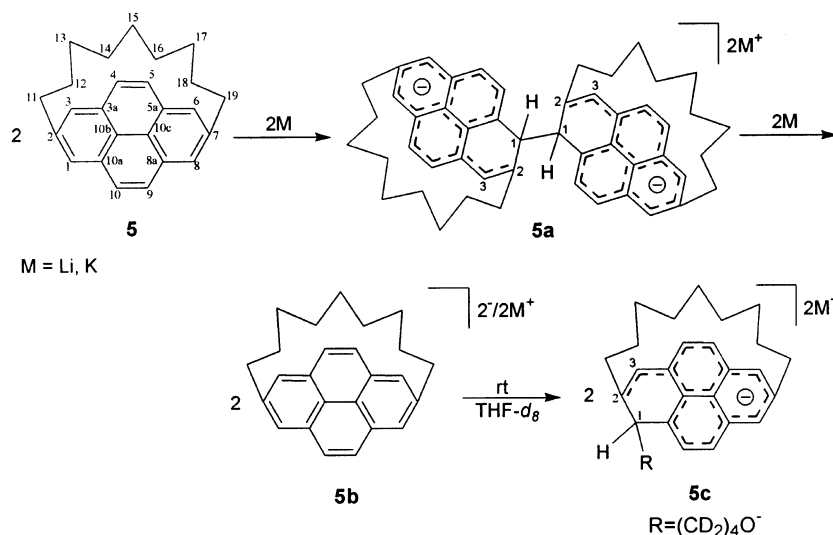
Another strong indication of the anti-aromaticity of the new species comes from the chemical shift of the tether hydrogens,

(24) The broadening is a result of the low temperature and dynamics, and thus the signals of these two hydrogen atoms are split into two broad peaks. For the sake of clarity, the average chemical shift of these broad peaks is used (this should correspond to the species with higher symmetry that cannot be observed clearly at low temperatures).

(25) Unfortunately, even at 165 K hydrogen atom **H1** in **2b** and **3b** appears as a broad singlet, and no splitting is seen. Such a splitting might have made the observation of the direct coupling between **H1** and **H3** possible.

(26) The presence of a dynamic process in the compound lowers its symmetry, and thus the signals of these two hydrogen atoms are split into two broad peaks. For the sake of clarity, the average chemical shift of these broad peaks is used (this should correspond to the species with higher symmetry that cannot be observed clearly at low temperatures).

(27) Minsky, A.; Meyer, A. Y.; Poupko, R.; Rabinovitz, M. *J. Am. Chem. Soc.* **1983**, *105*, 2164.

Scheme 4. Diamagnetic Reduction Products Afforded from **5**

which function as probes for the anisotropy effect prevailing in the system. The effect is most notable at hydrogen atoms **H14** and **H14'**, where the latter absorbs at $\delta = 2.58$ ppm and the former, which feels the paramagnetic currents more strongly, absorbs at $\delta = 7.98$ ppm.²⁸ To the best of our knowledge, this is the first time that tether hydrogens have been used to probe the anti-aromaticity above the core of a polycyclic system.²⁹ It should be noted that the effect is more prominent in **5b/2K⁺** where **H14** and **H14'** absorb at $\delta = 9.93$ and 3.22 ppm, respectively.³⁰

The dynamic process of the tether, which also lowers the symmetry along it, was monitored using ¹H NMR spectroscopy. The signal of hydrogen atom **H10** in **5b** that appears as a singlet at 185 K ($\delta = 2.58$ ppm) broadens and is finally split into two broad singlets when the temperature is further lowered ($\delta = 2.61$ and 2.50 ppm at 165 K). The ΔG^\ddagger of the process was found to be 8.6 ± 0.2 kcal/mol,³¹ which is similar to the ΔG^\ddagger of the neutral system (8.8 ± 0.2 kcal/mol).³² This shows that the reduction has a minimal effect on the tether dynamics.

Quench experiments were not possible due to the instability of the species.

C. Third Reduction Product. The third reduction product, **5c** (wine-red when reduced with lithium and dark blue with potassium), can be obtained by heating the sample to room temperature. The third product has very similar ¹H and ¹³C NMR spectra to those of the dimer. In fact, except for some minor changes in the values of the chemical shifts, the spectra are almost identical. The only difference between the spectra is

detected via the proton-coupled HSQCSI experiment. Whereas a ³J_{H,*H} interaction is observed in the dimer, no such interaction exists for the new product,³³ which means that the rehybridization of carbon atom **C1** is not a result of dimerization. Nor does it occur through protonation, as happens in pyrene (**1a**, Scheme 1), because the integration of hydrogen atom **H1** shows the presence of only one hydrogen atom. More importantly the vicinal hydrogens in the protonation product are not equivalent and, thus, two doublets should be obtained, and this is not the case.

In the reduction process of **1**, the dianion (**1b**) cleaves the solvent (THF-*d*₈) upon heating to yield **1c** (Scheme 1).^{8c} This solvent cleavage affords a monoanionic pyrene moiety, in which the charge is concentrated on the phenalene subunit, and the reaction takes place at the same carbon atom as dimerization. This explains why only minor changes between the ¹H and ¹³C NMR spectra of two such products are to be expected. Based on this we assume that the new reduction product, **5c**, is that of solvent cleavage. Because the solvent used was deuterated, the carbon signals of the cleaved solvent are too weak to be observed (due to splitting of the carbons by the deuterium atoms).

Oxygen quench experiments conducted on **5c** afforded neutral **5**.

Tether of 10 Methylene Carbons: A. Synthesis. The synthesis of [10](2,7)pyrenophane (**6**) (Scheme 5) was conducted according to the synthetic pathway previously described for the syntheses of [7]-, [8]-, and [9](2,7)pyrenophanes.^{6c} Diestertriflate **8**^{6c} was subjected to a Sonogashira reaction with 1,9-decadiyne to afford diyne-tetraester **9** (68%), which was catalytically hydrogenated to give tetraester **10** (99%). Reduction of **10** with LiAlH₄ followed by treatment of the crude reaction mixture with HBr/HOAc led to the formation of tetrabromide **11** (66%). Reaction of **11** with Na₂S/Al₂O₃³⁴ provided dithiacyclophane **12** (78%). This was then converted into [10](2,7)pyrenophane by a standard series of five reactions without any purification

(28) The difference in absorption is a result of a dissimilarity in the orientation of the hydrogen atoms **H14** and **H14'** relative to the pyrene core.

(29) The ⁷Li NMR absorption of **5b/2Li⁺**, $\delta = 1.98$ ppm, shows the existence of solvent-separated ion pairs in the system and the presence of paramagnetic currents in the anion.

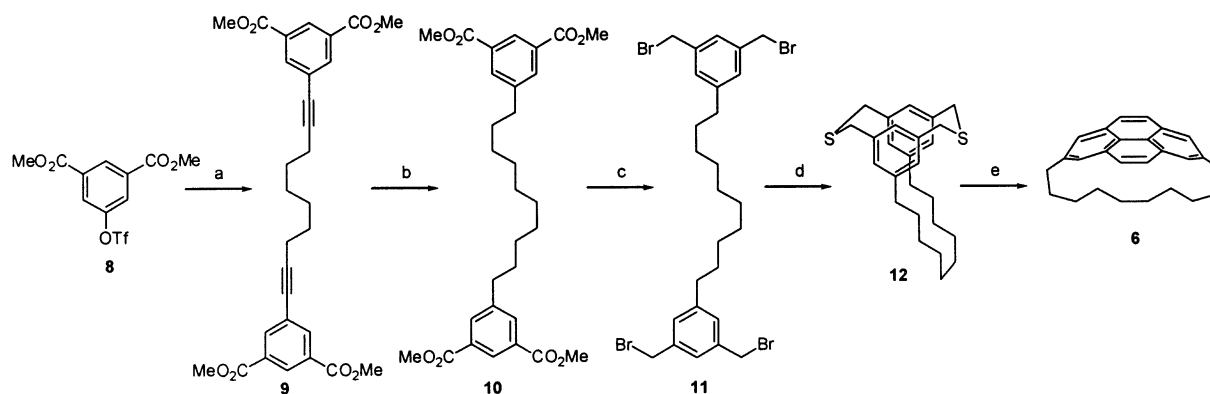
(30) The difference in $\Delta\delta$ ($\delta_{\text{H14}} - \delta_{\text{H14}'}$) between the lithium and potassium reduction products can be attributed to changes in the type of ion pairing in the system. Another indication of such a difference comes from the ¹³C NMR spectrum where carbon atom **C10b**, **C2**, and one of the **C1/3** carbons have a relatively large high-field shift in the lithium salt compared with the potassium salt. This shift can give an indication as to the location of the lithium cations relative to the anionic moiety.

(31) Due to the limitation in the available temperature range (THF freezes at 160 K), the ΔG^\ddagger value is only an approximation (higher limit), for it is not possible to measure the $\Delta\nu$ at the point of minimum or no exchange.

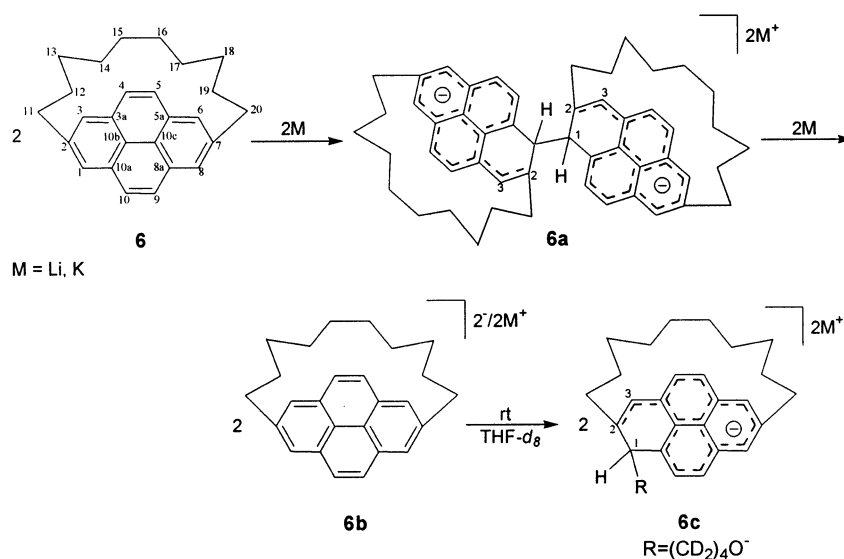
(32) A dynamic process was also observed in all the neutral compounds. Unpublished results.

(33) This experiment is of utmost importance, in addition to integration, it can help to distinguish between a number of products with similar NMR spectra.

(34) Bodwell, G. J.; Houghton, T. J.; Koury, H. E.; Yarlagadda, B. *Synlett* **1995**, 751.

Scheme 5. Synthesis of **6**^a

^a (a) 1,9-decadiyne, Pd(PPh₃)₂Cl, CuI, DBU, benzene, rt, 48 h, 68%; (b) H₂, Pd/C, EtOAc, rt, 16 h, 99%; (c) LiAlH₄, THF, reflux, 16 h, then 30% HBr/HOAc, reflux, 45 min, 66%; (d) Na₂S/Al₂O₃, 10% EtOH/CH₂Cl₂, rt, 16 h, 78%; (e) (MeO)₂CHBF₄, CH₂Cl₂, rt, 3 h, then *t*-BuOK, THF, rt, 16 h, then (MeO)₂CHBF₄, CH₂Cl₂, rt, 6 h, then *t*-BuOK, THF, rt, 6 h, then DDQ, benzene, rt, 22% from **12**.

Scheme 6. Diamagnetic Reduction Products Afforded from **6**

of intermediates. This involved the treatment of **12** with (MeO)₂CHBF₄ (Borch reagent)³⁵ and then *t*-BuOK to bring about a Stevens rearrangement, followed by Borch reagent and then *t*-BuOK to induce Hofmann elimination. This afforded a ca. 3:1 mixture of pyrenophane **6** and an unidentified dihydropyrene. Finally, reaction of this mixture with DDQ afforded **6** in 20% overall yield from **12**.

B. Reduction. The reduction of **6** (colorless) with lithium or potassium metal affords three diamagnetic reduction compounds (Scheme 6): (1) A dimer (**6a**) (wine-red); (2) an anti-aromatic species (**6b**) (brown-red when reduced with lithium and blue with potassium); and in the end, (3) a solvent cleavage product (**6c**) (wine-red when reduced with lithium and violet with potassium).

C. One-Electron Reduction. The first reduction compound is possibly a radical anion (orange solution with no ¹H NMR spectrum) that with time affords the insoluble dimer **6a**: The reduction product with lithium (**6a**/2Li⁺) produces a very weak and partial ¹H NMR spectrum, assigned according to the ¹H NMR spectrum of **6c** (no ¹³C NMR is available). When the compound is reduced with potassium (**6a**/2K⁺), only small

“humps” are seen in the appropriate region of the ¹H NMR spectrum.

D. Two-Electron Reduction. As is the case with **5**, the two-electron reduction of **6** yields an anti-aromatic species **6b**. The anti-aromaticity of the system manifests itself most notably at hydrogen atoms **H14** and **H14'**, which absorb at $\delta = 6.95$ and 2.38 ppm, respectively.²⁸ Again the effect is more noticeable in **6b**/2K⁺, where **H14** and **H14'** absorb at $\delta = 8.68$ and 3.10 ppm, respectively.³⁰

The ΔG^\ddagger of the tether dynamics, which lowers the symmetry along it, was measured for both **6** and **6b** by monitoring the temperature dependence of the absorption of hydrogen atom **H1** in **6** and hydrogen atom **H2** in **6b**. It was found that ΔG^\ddagger is 8.4 ± 0.2 and 8.9 ± 0.2 kcal/mol for **6** and **6b**,³¹ respectively. This again shows that the reduction has a minimal effect on the dynamic process.

E. Third-Reduction Product. The compound **6b** is not stable and eventually cleaves the solvent to afford **6c**. Quenching **6c** with oxygen gives neutral **6**.

Systems at Large: The reduction of the series of [*n*](2,7)-pyrenophanes (*n* = 7–10) shows the processes involved are not alkali metal-dependent. It is possible to generalize and state that as far as the single-electron reduction is concerned, the

(35) Borch, R. F. *J. Org. Chem.* **1969**, *34*, 627.

degree of strain in the system plays no crucial role. However, the product of the two-electron reduction is seen to depend on the strain in the system.

A. Dimerization. The first reduction process, reductive dimerization, is common to all the $[n](2,7)$ pyrenophanes studied. To explain why dimerization occurs, one should refer to the radical anion of **1**. It has been shown for **1** that position **C1** (and its symmetrical counterparts) has the highest spin density for the odd electron in the monoanion radical.³⁶ This explains the high reactivity of this site and the likelihood of it undergoing radical coupling.³⁷

Why is it then that **1** itself does not dimerize but is rather protonated? The difference between the two sets of systems is the alkane tether. This has the dual function of enforcing nonplanarity on the polycyclic aromatic portion of the systems and increasing their solubility, which is evident from the comparatively high solubility of all the neutral pyrenophanes studied.^{6c} It seems that curvature does not significantly alter the spin distribution in the radical anion of the pyrene moiety because dimerization in the $[n](2,7)$ pyrenophanes and protonation in **1** take place at the same carbon atom.

With regard to solubility, the effect of the tether on the systems is profound.³⁸ In our experiments some precipitate was seen along with the protonation product of **1**. The solubility of the precipitate increased with temperature, but no diamagnetic species other than the protonation product was observed in the NMR spectra. Müllen et al. previously reported that, at low temperatures, the radical anion of **1** might be in equilibrium with a diamagnetic dimer, which undergoes cleavage at higher temperatures.^{8c} In view of this, one may assume that a dimeric product might also be produced from **1** but is not observed by NMR spectroscopy due to low solubility.³⁹

It seems that although the tether contributes to the solubility of the neutral systems, its contribution to the solubility of the dimers is limited; the solubility of the dimer decreases as a function of tether length, i.e., as the pyrene system becomes less distorted.

The nonplanarity of the pyrene unit, induced by the tether, imparts an element of asymmetry to each half of the respective dimers. This leads to the possibility of generating diastereomeric reduced species. Even if one assumes that the new σ -bond forms on the less hindered *exo* faces of the pyrene moieties, two possible products still remain, a *meso* diastereomer and a *dl* pair. From the data available, only one diastereoisomer appears to dominate. Unfortunately, it is not possible to fully assign the relative stereochemistry of the dimers, although it is apparent from the $^3J_{\text{H},*\text{H}}$ coupling constants that they all adopt an anti conformation about the new σ -bond.

B. Two-Electron Reduction. Whereas in the first reduction process the length of the tether shows no influence on the nature of the reduction product, in the second reduction step, the

product depends on the length of the tether, i.e., strain. Compounds **5** and **6**, which have relatively long tethers, behave like **1**. Therefore, their two-electron reduction yields anti-aromatic species, **5b** and **6b**.

The surprising finding is that the strain in **2** and **3** brings about the formation of an intramolecular σ -bond as a means of avoiding an unfavorable strained dianionic anti-aromatic state. The new σ -bond has a dual function: First, it releases some of the strain in the pyrene moiety by producing a “cyclopropyl” anion, which because of its geometrical requirements introduces a pronounced fold into what was the pyrene moiety, leaving behind a relatively flat aromatic “phenalenyl” anion.⁴⁰ Second, it provides a means of separating the two charges, thus allowing the system to avoid acquiring anti-aromatic character by sacrificing the benzene ring.

The threshold is a tether of eight carbon atoms where no two-electron reduction occurs. It seems that the strain in **4** is large enough that it does not get into an anti-aromatic state. Moreover, it seems that the formation of an intramolecular σ -bond is not favored either, because insufficient stabilization is gained in this way (the amount of strain is not large enough).

Whereas **2** and **3** yield two reduction products, **5** and **6** have an additional step in the reduction process. The solvent cleavage of **5b** and **6b** is a result of the nature of the anti-aromatic species. The solvent cleavage affords a monoanionic pyrene entity, in which the phenalenyl anion motif can be easily recognized (see **5c** and **6c**, Schemes 4 and 5). Thus, by attacking the solvent, the system transforms from an anti-aromatic to an aromatic species. Again it should be noted that the attack is at carbon atom **C1**, as this carbon has the highest density of charge on it in the dianionic state.^{8c}

The similarity in the behavior of **1**, **5**, and **6** upon reduction strengthens the hypothesis that dimerization may indeed occur in pyrene itself.

Conclusions

The reduction with alkali metals of a series of $[n](2,7)$ -pyrenophanes ($n = 7-10$), in which the strain in the system is controlled by the length of the tether, shows that the process can be divided into two steps. The first step, which is common to all the compounds, is a reductive dimerization process via electron coupling. The dimers formed in this process contain an aromatic phenalenyl anion subunit. In the second step, the reduction product depends on the length of the tether. The threshold is a tether of eight carbons, where no two-electron reduction occurs. Molecules with longer tethers behave like pyrene and produce anti-aromatic anions that can cleave the solvent at room temperature. Pyrenophanes with shorter tethers tend to form an intramolecular σ -bond to avoid a state of strained anti-aromaticity. The new σ -bond has two functions: lowering the relative strain in the system and separating the aromatic phenalenyl anion and the second added electron.

The fact that compounds **5** and **6** behave like pyrene when reduced with alkali metals and the presence of solubility problems in dimers with large tethers suggest that a dimerization process might also be possible in pyrene. The difficulty in observing such a dimer may lie in its low solubility.

(36) Hoijtink, G. J.; Townsend, J.; Weissman, S. I. *J. Chem. Phys.* **1961**, *34*, 507.

(37) Further support comes from the calculation of the atomic-orbital coefficients of the LUMO of **2** that contains the most strained pyrene moiety. DFT calculations (B3LYP/6-311G**) predict a high spin density for the odd electron in the monoanion radical of **2** at carbon atom **C1** and its symmetrical counterparts.

(38) The contribution of nonplanarity to the solubility of the systems is not well understood. Because nonplanarity is a function of tether length, the discussion on solubility will only focus on the latter, which indirectly contains the effect of the former.

(39) Such a reduction process has been observed in azulene. See ref 14b.

(40) Sethson, I.; Johnels, D.; Edlund, U.; Sygula, A. *J. Chem. Soc., Perkin Trans. 2* **1990**, 1339.

The use of the proton-coupled HSQCSI method was crucial in this study as it helped differentiate between the diverse reduction products.

Experimental Section

The 1D and 2D NMR spectra were recorded on a Bruker DRX-400 pulsed FT spectrometer operating at 400.13, 100.62, and 155.51 MHz for ^1H , ^{13}C , and ^7Li NMR, respectively. Chemical shifts were measured relative to the most downfield solvent peak (THF- d_8 3.57 ppm relative to TMS). Coupling constants are reported whenever they are essential. The temperature was calibrated with methanol.

The assignment of the tether hydrogen atoms is conducted as follows: the tether hydrogen showing a NOESY (Nuclear Overhauser Effect Spectroscopy) interaction with hydrogen atom **H1**, which belongs to the pyrene moiety, is assigned as **H11**. This hydrogen atom will show a COSY interaction with hydrogen atom **H11'** (if these atoms are not equivalent) and a secondary interaction with hydrogen atom **H12**. The rest of the hydrogen atoms are assigned following this sequence, using the COSY interactions. In some cases no integration data is given, because integration of the tether hydrogens was not possible due to overlapping or to their lying under the solvent peaks.

For the synthetic work, reactions were performed under nitrogen unless otherwise indicated. Solvents designated as dry were purified and dried using standard procedures. Spectroscopic grade benzene was degassed under reduced pressure immediately prior to use. All other solvents were used as received. Chromatographic separations were performed using 230–400 mesh silica gel. TLC plates were visualized using a short wave (254 nm) UV lamp. Melting points are uncorrected. ^1H and ^{13}C NMR were acquired using CDCl_3 solutions at 500 MHz and 125 MHz, respectively. Reported multiplicities are apparent. Low- and high-resolution EI mass spectroscopic data were obtained at 70 eV.

Reduction of the Samples. All [*n*](2,7)pyrenophanes were reduced in 5 mm NMR glass tubes equipped with an upper reduction chamber. The pyrenophanes (3–5 mg) were introduced into the lower chamber of the tube under argon atmosphere. The alkali metal (kept in paraffin oil, cleansed from the oxidized layer and rinsed in petroleum ether 40–60 °C) was introduced under argon to the reduction chamber as a lithium wire or a piece of potassium. The tube was then placed under high vacuum and dried by flame. In the case of potassium, the metal was sublimed several times, creating a potassium mirror on the reduction chamber. Approximately 1 mL of anhydrous THF- d_8 (dried over a sodium/potassium alloy under high vacuum) was vacuum-transferred to the NMR tube and was degassed several times. Finally the tube was flame-sealed under high vacuum.

Controlled Reduction Process. The reduction takes place when the THF- d_8 solution is brought into contact with the metal by inverting the sample in solid dry ice. Reduction is stopped by returning the sample to the upright position separating the metal from the solution. The formation of the anions was detected visually by the change in the color of the solution and by ^1H NMR spectroscopy.

Quench Reactions. Quenching with oxygen was performed under a nitrogen funnel. The sample tube was broken, and the reduction chamber containing the metal was removed. A mild stream of oxygen gas was bubbled through a syringe into the cooled solution until the color changed. Reaction with iodine and dimethyl sulfate was performed by breaking the sample tube (ca. 10 mg of substrate) in a glovebox and pouring the solution into a vial containing an appropriate amount of the reagent. The product was then extracted with dichloromethane and dried over magnesium sulfate, and the solvent was evaporated.

NMR Data. 2a/2Li⁺: δ_{H} (THF- d_8 , 200 K, wine-red) 6.63 (d, 1H, H4), 5.98 (d, 1H, H10), 5.95 (d, 1H, H9), 5.78 (s, 1H, H3), 5.71 (d, 1H, H5), 5.71 (s, 1H, H8), 5.62 (s, 1H, H6), 3.22 (s, 1H, $J_{\text{C,H}} = 128.23$ Hz, $J_{\text{H,H}} = 10.26$ Hz, H1), 2.45 (d, 1H, H17), 2.06 (d, 1H, H11), 1.80 (m, H17'), 1.57 (m, 1H, H11'), 1.40 (m, 1H, H16), 0.76 (m, 1H, H12),

0.62 (m, 1H, H16'), 0.35 (m, 1H, H15), 0.21 (m, 1H, H14), 0.08 (dd, 1H, H12'), -0.12 (t, 1H, H13 and H15'), -0.39 (dd, 1H, H13'), -0.60 (dd, 1H, H14') ppm. δ_{C} (THF- d_8 , 200 K) 142.66 (C8a), 142.19 (C5a), 140.56 (C10b), 138.85 (C10c), 135.48 (C7), 131.87 (C4), 129.75 (C10), 129.56 (C3), 119.28 (C6), 114.78 (C8), 110.65 (C3a), 110.04 (C9), 105.25 (C10a), 102.75 (C5), 99.41 (C2), 48.28 (C1), 40.74 (C11), 37.27 (C17), 34.55 (C14), 32.53 (C16), 31.50 (C12), 27.84 (C13), 25.09 (C15) ppm. δ_{Li} (THF- d_8 , 200 K) -0.63 ppm.

2a/2K⁺: δ_{H} (THF- d_8 , 260 K, dark-red) 6.73 (d, 1H, H4), 6.00 (d, 1H, H9), 5.94 (d, 1H, H10), 5.88 (s, 1H, H3), 5.87 (d, 1H, H5), 5.81 (s, 1H, H8), 5.73 (s, 1H, H6), 3.60 (s, 1H, $J_{\text{C,H}} = 130.52$ Hz, $J_{\text{H,H}} = 11.52$ Hz, H1), 2.48 (dd, 1H, H17), 2.15 (d, 1H, H11), 1.77 (m, H17'), 1.61 (t, 1H, H11'), 1.42 (b, 1H, H16), 0.85 (b, 1H, H12), 0.67 (b, 1H, H16'), 0.42 (b, 1H, H15), 0.23 (b, 1H, H14), 0.16 (dd, 1H, H12'), -0.10 (b, 1H, H13), -0.20 (t, 1H, H15') -0.48 (m, 1H, H13'), -0.57 (m, 1H, H14') ppm. δ_{C} (THF- d_8 , 260 K) 143.71 (C8a), 142.09 (C5a), 140.93 (C10b), 136.25 (C7), 135.85 (C10c), 132.71 (C4), 131.07 (C3), 129.11 (C10), 120.53 (C6), 115.83 (C8), 111.56 (C3a), 110.04 (C9), 104.55 (C5), 104.10 (C10a), 100.61 (C2), 50.68 (C1), 40.53 (C11), 37.18 (C17), 34.39 (C14), 32.28 (C16), 31.94 (C12), 27.89 (C13), 25.35 (C15) ppm.

2b/2Li⁺: δ_{H} (THF- d_8 , 273 K, wine-red) 6.18 (d, 1H, H10), 5.22 (d, 1H, H9), 5.06 (s, 1H, H8), 2.31 (s, 1H, $J_{\text{C,H}} = 163.16$ Hz, $J_{\text{H,H}} = 9.06$ Hz, H1), 2.00 (m, 1H, H17), 1.42 (m, 1H, H16), 1.21 (m, 1H, H11), 1.03 (m, 1H, H15), 0.82 (m, 1H, H12), 0.80 (m, 1H, H14), 0.71 (m, 1H, H13) ppm. δ_{C} (THF- d_8 , 273 K) 147.61 (C10b), 145.76 (C8a), 141.60 (C7), 136.94 (C10c), 125.66 (C10), 118.53 (C10a), 107.93 (C8), 101.60 (C9), 38.84 (C17), 33.92 (C1 and C13), 33.95 (C16), 32.76 (C11), 30.85 (C14), 29.26 (C15), 29.16 (C2), 27.99 (C12) ppm. δ_{Li} (THF- d_8 , 273 K) 0.16 ppm.

2b/2K⁺: δ_{H} (THF- d_8 , 260 K, brown) 6.20 (d, 1H, H10), 5.24 (d, 1H, H9), 5.05 (s, 1H, H8), 2.28 (s, 1H, $J_{\text{C,H}} = 162.44$ Hz, $J_{\text{H,H}} = 7.89$ Hz, H1), 1.98 (t, 1H, H17), 1.40 (b, 1H, H16), 1.17 (b, 1H, H11), 1.01 (b, 1H, H15), 0.80 (m, 1H, H12), 0.77 (m, 1H, H14), 0.71 (m, 1H, H13) ppm. δ_{C} (THF- d_8 , 273 K) 147.39 (C10b), 145.71 (C8a), 143.01 (C7), 136.52 (C10c), 126.29 (C10), 119.12 (C10a), 107.86 (C8), 102.13 (C9), 38.70 (C17), 33.84 (C1), 33.66 (C13), 32.82 (C16), 32.56 (C11), 30.77 (C14), 29.23 (C15 and C2), 27.85 (C12) ppm.

3a/2Li⁺: δ_{H} (THF- d_8 , 240 K, wine-red) 6.57 (m, 1H, H19), 6.56 (m, 1H, H18/H20), 6.29 (m, 1H, H18/H20), 6.26 (d, 1H, H4), 6.02 (d, 1H, H9), 5.91 (d, 1H, H10), 5.87 (s, 1H, H3), 5.82 (s, 1H, H8), 5.26 (d, 1H, H5), 5.24 (s, 1H, H6), 5.10 (s, 1H, H14), 3.41 (s, 1H, $J_{\text{C,H}} = 130.03$ Hz, $J_{\text{H,H}} = 10.60$ Hz, H1), 2.66 (q, 1H, H17), 2.47 (t, 1H, H11), 2.25 (m, 1H, H16'), 2.23 (m, 1H, H17'), 2.21 (m, 1H, H11'), 1.95 (d, 1H, H12'), 1.85 (m, 1H, H16), 1.45 (t, 1H, H12) ppm. δ_{C} (THF- d_8 , 240 K) 143.02 (C8a), 142.37 (C5a), 140.52 (C10b), 139.55 (C13/C15), 139.33 (C13/C15), 135.79 (C10c), 131.74 (C7), 129.80 (C4 and C14), 129.10 (C10), 129.00 (C3), 125.71 (C18/C20), 124.81 (C19), 124.21 (C18/C20), 118.28 (C6), 114.13 (C8), 113.08 (C3a), 109.34 (C9), 103.48 (C10a), 102.56 (C5), 95.74 (C2), 48.68 (C1), 40.22 (C16), 38.05 (C11), 37.95 (C17), 35.79 (C12) ppm. δ_{Li} (THF- d_8 , 240 K) -0.50 ppm.

3a/2K⁺: δ_{H} (THF- d_8 , 260 K, brown) 6.58 (t, 1H, H19), 6.51 (d, 2H, H18 and H20), 6.36 (d, 2H, H18 and H20), 6.51 (d, 1H, H4), 6.03 (d, 1H, H9), 5.94 (s, 1H, H3), 5.90 (s, 1H, H8), 5.88 (d, 1H, H10), 5.40 (d, 1H, H5), 5.36 (s, 1H, H6), 5.15 (s, 1H, H14), 3.67 (s, 1H, $J_{\text{C,H}} = 130.98$ Hz, $J_{\text{H,H}} = 10.80$ Hz, H1), 2.69 (q, 1H, H17), 2.55 (t, 1H, H11), 2.37 (dd, 1H, H16), 2.30 (m, 1H, H11'), 2.23 (m, 1H, H17), 1.99 (d, 1H, H12), 1.85 (m, 1H, H16), 1.49 (t, 1H, H12') ppm. δ_{C} (THF- d_8 , 260 K) 143.97 (C8a), 142.08 (C5a), 140.58 (C10b), 139.39 (C13/C15), 139.32 (C13/C15), 135.48 (C10c), 134.66 (C7), 132.37 (C4), 132.02 (C14), 130.35 (C3), 128.42 (C10), 125.89 (C18/C20), 124.93 (C19), 124.26 (C18/C20), 119.42 (C6), 115.21 (C8), 113.89 (C3a), 109.11 (C9), 104.67 (C5), 102.46 (C10a), 96.79 (C2), 51.29 (C1), 39.98 (C16), 37.88 (C17), 37.74 (C11), 36.17 (C12) ppm.

3b/2Li⁺: The ΔG^\ddagger for the dynamic process was measured to be 9.1 ± 0.2 kcal/mol.

δ_{H} (THF- d_8 , 260 K, brown-red) 6.83 (s, 1H, H14), 6.71 (t, 1H, H19), 6.60 (d, 1H, H18), 6.51 (d, 1H, H20), 6.17 (d, 2H, H10), 5.11 (d, 2H, H9), 4.82 (s, 2H, H8), 2.57 (t, 1H, H16), 2.39 (s, 2H, $J_{\text{C,H}} = 162.33$ Hz, $J_{\text{H,H}} = 8.66$ Hz, H1), 2.27 (t, 1H, H11), 2.20 (t, 1H, H17), 1.54 (t, 1H, H12) ppm. δ_{C} (THF- d_8 , 260 K) 146.95 (C10b), 146.09 (C13), 145.13 (C8a), 140.64 (C15), 140.52 (C7), 136.47 (C10c), 133.46 (C14), 126.23 (C19), 125.77 (C18), 125.58 (C10), 125.43 (C20), 118.07 (C10a), 108.47 (C8), 101.63 (C9), 39.92 (C16), 39.59 (C17), 33.71 (C1), 33.12 (C12), 32.97 (C11), 30.10 (C2). δ_{Li} (THF- d_8 , 260 K) -0.20 ppm.

3b/2K⁺: The ΔG^\ddagger for the dynamic process was measured to be 8.9 ± 0.2 kcal/mol.

δ_{H} (THF- d_8 , 273 K, brown) 6.85 (s, 1H, H14), 6.76 (t, 1H, H19), 6.64 (d, 1H, H18), 6.55 (d, 1H, H20), 6.25 (d, 1H, H10), 5.18 (d, 1H, H9), 4.86 (s, 1H, H8), 2.60 (t, 1H, H16), 2.42 (s, 1H, $J_{\text{C,H}} = 163.64$ Hz, $J_{\text{H,H}} = 8.12$ Hz, H1), 2.33 (t, 1H, H11), 2.22 (t, 1H, H17), 1.60 (t, 1H, H12) ppm. δ_{C} (THF- d_8 , 273 K) 146.78 (C10b), 145.90 (C13), 145.13 (C8a), 142.29 (C7), 140.37 (C15), 136.03 (C10c), 133.13 (C14), 126.59 (C19), 126.26 (C10), 125.63 (C18), 125.60 (C20), 118.98 (C10a), 108.27 (C8), 102.14 (C9), 39.72 (C16), 39.50 (C17), 33.80 (C1), 33.18 (C12), 32.85 (C11), 30.30 (C2) ppm.

4a/2Li⁺: δ_{H} (THF- d_8 , 273 K, wine-red) 6.58 (d, 1H, H4), 5.94 (dd, 2H, H9 and H10), 5.84 (s, 1H, H3), 5.76 (s, 1H, H8), 5.69 (s, 1H, H6), 5.67 (d, 1H, H5), 3.24 (s, 1H, H1, $J_{\text{C,H}} = 130.92$ Hz, $J_{\text{H,H}} = 10.61$ Hz), 2.45 (dd, 1H, H18), 2.22 (d, 1H, H11), 1.83 (dt, 1H, H18'), 1.60 (m, 2H, H11' and H17'), 1.03 (dd, 1H, H12), 0.86 (m, 2H, H16 and H17'), 0.63 (dd, 1H, H16'), 0.38 (dd, 1H, H12'), 0.23 (dd, 1H, H14), -0.01 (m, 2H, H13' and H15'), -0.26 (dd, 1H, H13), -0.50 (dd, 1H, H14'), -0.82 (dd, 1H, H15) ppm. δ_{C} (THF- d_8 , 273 K) 143.39 (C5a), 139.78 (C8a), 138.59 (C10b), 135.69 (C7), 135.31 (C10c), 131.15 (C4), 129.77 (C10), 129.13 (C3), 114.21 (C8), 111.57 (C3a), 110.16 (C6), 109.52 (C9), 108.51 (C10a), 103.31 (C2), 102.76 (C5), 49.07 (C1), 40.84 (C11), 38.37 (C18), 33.40 (C15), 32.23 (C12), 32.08 (C17), 31.91 (C14), 27.81 (C16), 27.13 (C13) ppm. δ_{Li} (THF- d_8 , 273 K) -0.70 ppm.

4a/2K⁺: δ_{H} (THF- d_8 , 240 K, wine-red) 6.66 (d, 1H, H4), 5.98 (d, 1H, H9), 5.88 (d, 1H, H10), 5.87 (s, 1H, H3), 5.83 (s, 1H, H8), 5.82 (s, 1H, H6), 5.81 (d, 1H, H5), 3.49 (s, 1H, $J_{\text{C,H}} = 130.58$ Hz, $J_{\text{H,H}} = 11.14$ Hz, H1), 2.46 (dd, 1H, H18), 2.28 (d, 1H, H11), 1.86 (m, 1H, H18'), 1.62 (d, 1H, H11'), 1.57 (d, 1H, H17'), 1.03 (d, 1H, H12), 0.85 (m, 1H, H15), 0.81 (m, 1H, H17'), 0.62 (t, 1H, H15'), 0.41 (dd, 1H, H12'), 0.27 (d, 1H, H13), -0.03 (m, 1H, H14 and H16), -0.38 (d, 1H, H16'), -0.44 (d, 1H, H13'), -1.04 (dd, 1H, H14') ppm. δ_{C} (THF- d_8 , 240 K) 142.87 (C5a), 140.17 (C8a), 138.85 (C10b), 136.09 (C7), 134.97 (C10c), 131.54 (C4), 129.85 (C3), 129.36 (C10), 114.89 (C8), 111.74 (C6), 111.24 (C3a), 109.14 (C9), 107.15 (C10a), 104.51 (C5), 103.57 (C2), 49.85 (C1), 40.69 (C11), 38.17 (C18), 32.48 (C14), 32.11 (C12), 31.96 (C17), 31.51 (C13), 27.76 (C15), 27.12 (C16) ppm.

5a/2Li⁺: δ_{H} (THF- d_8 , 240 K, wine-red) 6.33 (d, 1H, H4), 5.84 (s, 1H, H3), 5.81 (d, 1H, H10), 5.76 (d, 1H, H9), 5.58 (s, 1H, H8), 5.51 (d, 1H, H5), 5.45 (s, 1H, H6), 3.27 (s, 1H, $J_{\text{C,H}} = 130.64$ Hz, $J_{\text{H,H}} = 10.44$ Hz, H1), 2.39 (m, 1H, H11), 2.30 (m, 1H, H19), 1.95 (m, 1H, H19'), 1.91 (m, 1H, H11'), 1.42 (m, 1H, H18), 1.14 (m, 1H, H12), 1.08 (m, 1H, H18'), 0.87 (m, 3H, H12', H17, and H17'), 0.69 (m, 1H, H13'), 0.60 (m, 1H, H13), 0.27 (m, 2H, H15' and 16), 0.08 (m, 3H, H14, H15, and H16'), -0.14 (1H, H14') ppm. δ_{C} (THF- d_8 , 240 K) 142.59 (C5a), 140.94 (C8a), 136.58 (C10b), 135.89 (C7), 135.21 (C10c), 131.07 (C10), 128.89 (C4), 126.43 (C3), 112.85 (C10a), 112.53 (C3a), 111.75 (C6), 108.73 (C8 and C9), 106.84 (C2), 102.18 (C5), 52.39 (C1), 40.85 (C11), 37.65 (C19), 34.13 (C14), 33.73 (C16), 32.42 (C15), 30.84 (C18), 30.75 (C12), 27.01 (C17), 26.66 (C13) ppm. δ_{Li} (THF- d_8 , 240 K) -0.69 ppm.

5a/2K⁺: δ_{H} (THF- d_8 , 220 K, wine-red) 6.40 (d, 1H, H4), 5.88 (s, 1H, H3), 5.84 (d, 1H, H9), 5.74 (d, 1H, H10), 5.65 (s, 1H, H8), 5.60 (d, 1H, H5), 5.54 (s, 1H, H6), 3.36 (s, 1H, H1, $J_{\text{C,H}} = 132.05$ Hz, $J_{\text{H,H}} = 10.15$ Hz), 2.44 (m, 1H, H11), 2.33 (m, 1H, H19), 1.95 (m, 1H, H19'/H11'), 1.89 (m, 1H, H11'/H19'), 1.43 (m, 1H, H18), 1.21 (m,

1H, H12), 1.08 (m, 1H, H18'), 0.89 (m, 1H, H17'/H12'), 0.88 (m, 1H, H17), 0.87 (m, 1H, H12'/H17'), 0.74 (m, 1H, H13'), 0.61 (m, 1H, H13), 0.28 (m, 2H, H15' and 16), 0.10 (m, 3H, H14, H15, and H16'), -0.11 (m, 1H, H14') ppm. δ_{C} (THF- d_8 , 220 K) 142.56 (C5a), 141.31 (C8a), 136.95 (C7), 136.75 (C10b), 134.98 (C10c), 131.27 (C10), 129.42 (C4), 126.30 (C3), 112.20 (C6), 112.20 (C3a), 109.64 (C8), 108.94 (C9), 108.31 (C10a), 108.31 (C2), 102.43 (C5), 52.98 (C1), 40.63 (C11), 37.57 (C19), 34.06 (C14), 33.60 (C16), 32.41 (C15), 30.66 (C18), 29.87 (C12), 27.02 (C17), 26.75 (C13) ppm.

5b/2Li⁺: The ΔG^\ddagger for the dynamic process was measured to be 8.6 ± 0.2 kcal/mol.

δ_{H} (THF- d_8 , 165 K, brown-red) 7.98 (b, 2H, H14), 4.61 (b, 1H, H15'), 3.55 (H13'), 2.61 (s, 2H, H4/H10), 2.58 (b, H14'), 2.50 (s, 2H, H4/H10), 2.43 (b, 1H, H15), 2.14 (b, 4H, H12' and H13), 1.95 (b, 2H, H12), 1.57 (s, 2H, H1/H3), 1.29 (s, 2H, H1/H3), 0.96 (b, 2H, H11), 0.83 (b, 2H, H11') ppm. δ_{C} (THF- d_8 , 165 K) 151.91 (C10b), 144.28 (C3a/C10a), 143.40 (C3a/C10a), 137.46 (C2), 108.53 (C3/C4), 107.68 (C3/C4), 98.04 (C1/C3), 83.74 (C1/C3), 38.12 (C11), 37.89 (C14), 36.20 (C15), 32.77 (C12), 29.39 (C13) ppm. δ_{Li} (THF- d_8 , 165 K) 1.98 ppm. Carbon atoms C10b and C2 were assigned according to the ^{13}C NMR of **1b**. The differentiation between hydrogen and carbon atoms C1 and C3 (also C4 and C10) is not possible.

5b/2K⁺: The ΔG^\ddagger for the dynamic process was measured to be 8.6 ± 0.2 kcal/mol.

δ_{H} (THF- d_8 , 170 K, blue) 9.93 (b, 2H, H14), 8.65 (b, 1H, H15'), 4.01 (b, 2H, H13'), 3.22 (b, 2H, H14'), 2.89 (b, 1H, H15), 2.41 (b, 2H, H13), 2.34 (b, 2H, H12'), 2.04 (b, 2H, H12), 1.89 (s, 2H, H4/H10), 1.83 (s, 2H, H4/H10), 0.99 (s, 2H, H1/H3), 0.89 (s, 2H, H1/H3), 0.64 (b, 2H, H11), 0.56 (b, 2H, H11') ppm. δ_{C} (THF- d_8 , 170 K) 156.66 (C10b), 145.02 (C3a/C10a), 144.60 (C3a/C10a), 141.70 (C2), 107.71 (C3/C4), 106.89 (C3/C4), 98.47 (C1/C3), 89.71 (C1/C3), 39.17 (C14), 37.89 (C11), 37.34 (C15), 33.77 (C13), 30.60 (C12) ppm. Carbon atoms C10b and C2 were assigned according to the ^{13}C NMR of **1b**. The differentiation between hydrogen and carbon atoms C1 and C3 (also C4 and C10) is not possible.

5c/2Li⁺: δ_{H} (THF- d_8 , 273 K, dark-blue) 6.33 (d, 1H, H4), 6.24 (d, 1H, H10), 6.05 (d, 1H, H9), 5.78 (s, 1H, H3), 5.77 (s, 1H, H8), 5.59 (s, 1H, H6), 5.58 (d, 1H, H5), 2.83 (s, 1H, $J_{\text{C,H}} = 122.36$ Hz, H1), 2.38 (m, 1H, H19), 2.08 (m, 1H, H11), 1.98 (m, 1H, H19'), 1.90 (m, 1H, H11'), 1.42 (m, 1H, H18'), 1.27 (m, 1H, H12), 1.14 (m, 1H, H18), 0.89 (m, 1H, H17'), 0.86 (m, 3H, H12, H17 and H17'), 0.68 (m, 1H, H13), 0.53 (m, 1H, H13'), 0.26 (m, 1H, H15), 0.21 (m, 1H, H14'), 0.18 (m, 1H, H16), 0.07 (m, 2H, H15' and H16'), 0.03 (m, 1H, H14) ppm. δ_{C} (THF- d_8 , 273 K) 142.25 (C5a), 141.40 (C8a), 136.23 (C10b), 136.08 (C7), 135.15 (C10c), 129.76 (C4), 128.03 (C10), 126.99 (C3), 112.99 (C6), 111.26 (C3a), 110.45 (C8), 110.16 (C9), 108.33 (C10a), 104.05 (C2), 103.55 (C5), 48.95 (C1), 39.54 (C11), 37.54 (C19), 33.80 (C14), 33.51 (C16), 32.50 (C15), 30.80 (C18), 30.62 (C12), 27.15 (C17), 26.61 (C13) ppm. δ_{Li} (THF- d_8 , 273 K) 0.05 ppm.

5c/2K⁺: δ_{H} (THF- d_8 , 298 K, dark-blue) 6.40 (d, 1H, H4), 6.35 (d, 1H, H10), 6.14 (d, 1H, H9), 5.87 (s, 1H, H3), 5.79 (s, 1H, H8), 5.63 (d, 1H, H5), 5.61 (s, 1H, H6), 3.17 (s, 1H, $J_{\text{C,H}} = 122.96$ Hz, H1), 2.38 (m, H19), 2.14 (m, H11), 2.03 (m, H19'), 1.93 (m, H11'), 1.47 (m, H18'), 1.30 (m, H12), 1.15 (m, H18), 0.97 (m, H17'), 0.90 (m, H12'), 0.85 (m, H17), 0.77 (m, H13'), 0.58 (m, H13), 0.36 (m, H15'), 0.24 (m, H16'), 0.20 (m, H14'), 0.16 (m, H15), 0.14 (m, H16), -0.02 (m, H14) ppm. δ_{C} (THF- d_8 , 298 K) 142.64 (C5a), 141.98 (C8a), 138.30 (C7), 136.31 (C10b), 135.03 (C10c), 130.25 (C4), 129.16 (C10), 126.84 (C3), 112.47 (C6), 112.05 (C3a), 110.79 (C9), 110.00 (C8), 109.60 (C10a), 107.34 (C2), 103.07 (C5), 50.50 (C1), 39.42 (C11), 37.58 (C19), 33.93 (C14), 33.64 (C16), 32.54 (C15), 30.89 (C18), 30.35 (C12), 27.27 (C17), 26.84 (C13) ppm.

6: Synthesis. A. 1,10-Bis(3,5-bis(methoxycarbonyl)phenyl)-1,9-decadiyne (9). A mixture of 3,5-bis(methoxycarbonyl)phenyl triflate **8^{cc}** (8.18 g, 23.9 mmol), DBU (4.93 mL, 9.03 g, 59.4 mmol), 1,9-decadiyne (2.14 mL, 1.67 g 11.4 mmol), CuI (0.45 g, 2.4 mmol), and

Pd(PPh₃)₂Cl₂ (0.35 g, 0.50 mmol) in benzene (250 mL) was stirred at room temperature for 48 h. The reaction mixture was washed with 1 M aqueous HCl solution, water, and saturated aqueous NaCl solution. The organic layer was dried over MgSO₄, filtered, and concentrated under reduced pressure to afford an oily brown solid. Column chromatography (CH₂Cl₂) afforded **9** as a light brown solid (4.21 g, 68%). Mp 127.5–129 °C (95% ethanol); δ_H (CDCl₃) 8.55 (s, 2H), 8.22 (s, 4H), 3.94 (s, 12H), 2.46–2.44 (m, 4H), 1.67–1.65 (m, 8H); δ_C (CDCl₃) 166.2, 136.9, 131.2, 129.8, 125.5, 100.0, 93.0, 79.4, 52.9, 28.8, 19.8; EI-MS *m/z* (%) 518 (100, M⁺), 490 (33), 475 (14), 464 (10), 427 (14), 399 (9), 395 (4), 357 (3), 311 (8), 228 (17), 200 (8), 155 (9), 115 (13). HRMS: calcd for C₃₀H₃₀O₈ 518.1941, found 518.1948.

B. 1,10-Bis(3,5-bis(methoxycarbonyl)phenyl)decane (10). A mixture of diynetetraester **9** (2.05 g, 3.95 mmol) in EtOAc (100 mL) was purged with nitrogen gas for 20 min, and then 10% Pd/C (0.050 g) was added. The resulting mixture was stirred under an atmosphere of hydrogen (balloon) for 16 h. The reaction mixture was filtered through a plug of Celite, and the filtrate was concentrated under reduced pressure to yield **10** as a white solid (2.05 g, 99%). Mp 99–100 °C (95% ethanol); δ_H (CDCl₃) 8.50 (s, 2H), 8.05 (s, 4H), 3.94 (s, 12H), 2.70 (t, *J* = 8.1 Hz, 4H) 1.66–1.63 (m, 4H), 1.31–1.25 (br s, 12H); δ_C (CDCl₃) 166.9 144.2, 134.2, 130.9, 128.6, 52.7, 36.0, 31.6, 29.9, 29.8, 29.6; EI-MS *m/z* (%) 526 (32, M⁺), 494 (69), 462 (100), 430 (46), 401 (36), 398 (3), 342 (3), 232 (20), 207 (42), 189 (40), 149 (27), 119 (18), 105 (11). HRMS: calcd for C₃₀H₃₈O₈ 526.2567, found 526.2560.

C. 1,10-Bis(3,5-bis(bromomethyl)phenyl)decane (11). To a stirred slurry of LiAlH₄ (4.61 g, 122 mmol) in THF (150 mL) was added by syringe over 1 h a solution tetraester **10** (4.36 g, 8.28 mmol) in THF (100 mL). The resulting gray slurry was brought to a gentle reflux for 16 h. The reaction mixture was cooled on an ice bath and then quenched by the careful addition of EtOAc (200 mL) and then 1 M aqueous HCl solution (100 mL). The resulting mixture was stirred for a further 1 h. The layers were separated, and the aqueous layer was extracted with EtOAc. The combined organic layers were washed with saturated aqueous NaCl solution, dried over MgSO₄, filtered, and concentrated under reduced pressure to yield a white solid. To this was added a mixture of glacial acetic acid (125 mL) and 30% HBr/HOAc (7.04 mL, 33.2 mmol HBr), and the resulting brown mixture was heated at reflux for 45 min. The reaction mixture was cooled and poured into water (50 mL) and extracted with CH₂Cl₂. The combined organic layers were washed with saturated aqueous NaHCO₃ solution, water, and saturated aqueous NaCl solution. The organic layer was dried over MgSO₄, filtered, and concentrated under reduced pressure to yield a brown oil. Column chromatography (35% CH₂Cl₂/hexanes) afforded tetrabromide **11** (3.25 g, 66%) as a white solid. Mp 97–98 °C (toluene/heptane); δ_H (CDCl₃) 7.22 (s, 2H), 7.13 (s, 4H), 4.40 (s, 8H), 2.55 (t, *J* = 8.0 Hz, 4H), 1.62–1.56 (m, 4H), 1.27 (br s, 12H); δ_C (CDCl₃) 144.6, 138.5, 129.5, 127.2, 35.9, 33.4, 29.7, 29.5, 26.3; EI-MS *m/z* (%) M⁺ not observed. Satisfactory HRMS for this compound was not obtained.

D. 18,27-Dithia[10.3.3](1,3,5)cyclophane (12). To an efficiently magnetically stirred solution of tetrabromide **11** (2.78 g, 4.17 mmol) in 10% EtOH/CH₂Cl₂ (700 mL) under air was added Na₂S/Al₂O₃ (5.56 g, 13.6 mmol) in four roughly equal portions over 45 min. The resulting milky mixture was stirred for a further 16 h. The resulting mixture was gravity filtered, and the filtrate was concentrated under reduced pressure to afford a pale yellow solid. Flash chromatography (CH₂Cl₂) of the residue afforded dithiacyclophane **12** (1.34 g, 78%) as a white solid. Mp 175–177 °C (toluene/heptane); δ_H (CDCl₃) 7.13 (s, 2H), 6.63 (s, 4H), 3.84 (d, *J* = 14.8, 4H), 3.78, (d, *J* = 14.9, 4 H), 2.33–2.30 (m, 4H), 1.54–1.47 (m, 4H), 1.39–1.29 (m 12 H); δ_C (CDCl₃) 143.1, 137.6, 129.2, 127.1, 39.4, 35.9, 29.9, 28.9, 27.0, 26.7. EI-MS *m/z* (%) 411 (24), 410 (100, M⁺), 346 (39), 158 (62), 145 (31), 119 (54), 105 (33), 91 (41). HRMS: calcd for C₂₆H₃₄S₂ 410.2102, found 410.2111.

E. [10](2,7)Pyrenophane (6). To a solution of dithiacyclophane **12** (1.34 g, 3.26 mmol) in dry dichloromethane (30 mL) was added dropwise Borch reagent ((MeO)₂CHBF₄) (1.10 g, 6.85 mmol) over a period of 15 min. The reaction was then stirred for a further 3 h. The reaction mixture was concentrated under reduced pressure, and the resulting residue was stirred for 10 min with ethyl acetate (10 mL). The solvent was removed by decantation, and the resulting gummy pink solid was dried in vacuo until a fine pink powder was obtained. This was slurried in dry THF (30 mL), and to this stirred mixture was added *t*-BuOK (1.68 g, 14.8 mmol). The resulting brown mixture was stirred for 16 h. Concentration of the reaction mixture gave a brown oil, which was taken up in dichloromethane and passed through a short column of silica gel to afford a yellow oil. This oil was dissolved in dry dichloromethane (30 mL), and Borch reagent (0.915 g, 5.72 mmol) was added dropwise over a period of 15 min. The mixture was stirred for 6 h, and the solvent was removed under reduced pressure and dried in vacuo to yield a sticky brown solid. To the resulting residue was added dry THF (30 mL) and then *t*-BuOK (1.55 g, 13.7 mmol), and the resulting mixture was stirred for 6 h. The reaction mixture was concentrated under reduced pressure to afford a brown solid. Column chromatography (25% CH₂Cl₂/hexanes) afforded a ca. 3:1 mixture of [10](2,7) pyrenophane and an unidentified [10](2,7)dihydropyrenophane. This mixture was dissolved in distilled benzene (25 mL), and to the resulting solution was added DDQ (0.056 g, 0.33 mmol). The resulting mixture was heated at reflux for 3 h, cooled to room temperature, and quenched by the addition of a few crystals of 1,4-hydroquinone. Column chromatography (hexanes) afforded pyrenophane **6** (0.225 g, 20% from **12**) as a white solid. Mp 253–255 °C (hexanes); δ_H (CDCl₃) 7.96 (s, 4H), 7.87 (s, 4H) 2.99–2.96 (m, 4H), 1.54–1.40 (m, 4H), 0.46–0.44 (m, 4H), –1.03, –1.04 (m, 4H), –1.70 (br s, 4H); δ_C (CDCl₃) 137.4, 131.1, 129.0, 127.6, 126.8, 35.9, 31.5, 31.4, 25.7, 23.4; EI-MS *m/z* (%) 340 (100, M⁺), 279 (2), 228 (36), 215, (22), 202, (3), 149 (18). HRMS: calcd for C₂₆H₂₈ 340.2191, found 340.2189.

6: The Δ*G*[‡] for the dynamic process was measured to be 8.3 ± 0.2 kcal/mol. δ_H (THF-*d*₈, 273 K, colorless) 7.98 (s, 1H, H10), 7.93 (s, 1H, H1), 2.97 (t, 1H, H11), 1.40 (dt, 1H, H12), 0.46 (m, 1H, H13), –1.07 (b, 1H, H15), –1.13 (b, 1H, H14) ppm. δ_C (THF-*d*₈, 298 K) 138.58 (C2), 132.09 (C10a), 128.24 (C1), 127.76 (C10), 125.63 (C10b), 36.87 (C11), 31.98 (C15), 31.34 (C14), 30.51 (12), 26.32 (C13) ppm.

6a/2Li⁺: δ_H (THF-*d*₈, 220 K, wine-red) 6.02 (d, 1H, H4), 5.85 (d, 1H, H10), 5.56 (s, 1H, H9), 5.49 (s, 1H, H3), 5.42 (s, 1H, H8), 5.31 (d, 1H, H6), 3.45 (s, 1H, H5), 2.40 (b, 1H, H20), 2.26 (b, 1H, H11) ppm. Assigned according to ¹H NMR spectrum of **6c**.

6b/2Li⁺: The Δ*G*[‡] for the dynamic process was measured to be 8.9 ± 0.2 cal/mol. δ_H (THF-*d*₈, 165 K, brown-red) 6.95 (b, 1H, H14), 4.99 (b, 1H, H15'), 2.91 (b, 1H, H13'), 2.70 (b, 1H, H4/H10), 2.55 (b, 1H, H4/H10), 2.38 (b, 2H, H14' and H15), 1.92 (H13), 1.77 (H1/H3), 1.67 (H12'), 1.57 (H12), 1.11 (b, 1H, H1/H3), 0.68 (b, 1H, H11), 0.54 (b, 1H, H11') ppm. δ_C (THF-*d*₈, 165 K) 151.02 (C10b), 149.27 (C3a/C10a), 139.17 (C3a/C10a), 138.56 (C2), 110.79 (C4/C10), 106.73 (C4/C10), 101.08 (C1/C3), 79.83 (C1/C3), 37.55 (C11), 36.54 (C14 and C15), 30.30 (C12), 28.61 (C13) ppm. δ_{Li} (THF-*d*₈, 165 K) 1.16 ppm. The differentiation between hydrogen and carbon atoms C1 and C3 (also C4 and C10) is not possible. Carbon atoms C10b and C2 were assigned according to the ¹³C NMR of **1b**.

6b/2K⁺: The Δ*G*[‡] for the dynamic process was measured to be 8.4 ± 0.2 kcal/mol. δ_H (THF-*d*₈, 165 K, blue) 8.68 (b, 1H, H14), 6.60 (b, 1H, H15'), 3.54 (b, 1H, H13'), 3.10 (b, 1H, H14'), 2.97 (b, 1H, H15), 2.14 (b, 1H, H13), 1.81 (b, 1H, H4/H10), 1.75 (b, 1H, H12'), 1.61 (b, 1H, H4/H10), 1.53 (b, 1H, H12), 0.87 (b, 1H, H1/H3), 0.64 (b, 1H, H1/H3), 0.24 (b, 1H, H11), 0.18 (b, 1H, H11') ppm. δ_C (THF-*d*₈, 298 K) 156.02 (C10b), 148.92 (C3a/C10a), 142.33 (C2 and C10a/C3a), 109.06 (C4/C10), 106.63 (C4/C10), 99.19 (C1/C3), 88.65 (C1/C3), 38.05 (C14), 37.79 (C15), 36.60 (C11), 31.06 (C12), 28.95 (C13) ppm. The differentiation between hydrogen and carbon atoms C1 and C3 (also C4 and C10) is not possible.

6c/2Li⁺: δ_{H} (THF-*d*₈, 273 K, wine-red) 6.19 (d, 1H, H4), 6.17 (d, 1H, H10), 5.98 (d, 1H, H9), 5.75 (s, 1H, H3), 5.66 (s, 1H, H8), 5.58 (s, 1H, H6), 5.49 (d, 1H, H5), 3.24 (s, 1H, $J_{\text{C,H}} = 122.63$ Hz, H1), 2.44 (m, 1H, H20), 2.37 (m, 1H, H11), 1.87 (m, 1H, H20'), 1.74 (1H, H11'), 1.58 (H19), 1.50 (H12), 1.17 (H13), 1.17 (H19'), 1.02 (H12'), 0.99 (17), 0.94 (13'), 0.64 (1H, H17'), 0.60–0.40 (m, 6H, H14, H15, H16, H16', H18, and H18'), 0.32 (1H, H14'), 0.06 (m, 1H, H15') ppm. δ_{C} (THF-*d*₈, 298 K) 142.98 (C5a), 140.40 (C8a), 136.77 (C7), 135.53 (C10b), 134.86 (C10c), 128.34 (C4/C10), 128.27 (C4/C10), 126.27 (C3), 111.00 (C10a and C8), 110.47 (C3a), 109.23 (C2), 109.11 (C9), 107.60 (C6), 103.32 (C5), 46.49 (C1), 39.47 (C11), 38.02 (C20), 33.26 (C13), 32.78 (C14), 32.67 (C15), 32.23 (C18), 30.81 (C19), 28.16 (C12), 27.57 (C13), 27.04 (C17) ppm. δ_{Li} (THF-*d*₈, 273 K) 0.04 ppm.

6c/2K⁺: δ_{H} (THF-*d*₈, 273 K, violet) 6.26 (d, 1H, H10), 6.24 (d, 1H, H4), 6.05 (d, 1H, H9), 5.80 (s, 1H, H3), 5.66 (s, 1H, H8), 5.58 (s, 1H, H6), 5.51 (d, 1H, H5), 3.21 (s, 1H, $J_{\text{C,H}} = 124.44$ Hz, H1), 2.40 (m, 1H, H20), 2.39 (m, 1H, H11), 1.89 (m, 1H, H20'), 1.81 (m, 1H,

H11'), 1.61 (m, 1H, H19), 1.48 (m, 1H, H12), 1.19 (m, 1H, H13), 1.16 (m, 1H, H19'), 1.07 (m, 1H, H12'), 1.04 (m, 1H, H17), 0.94 (m, 1H, H13'), 0.65 (m, 1H, H17'), 0.60–0.40 (m, 6H, H14, H15, H16, H16', H18 and H18'), 0.39 (m, 1H, H14'), 0.11 (m, 1H, H15') ppm. δ_{C} (THF-*d*₈, 273 K) 143.34 (C5a), 140.80 (C8a), 138.59 (C7), 135.67 (C10b), 134.79 (C10c), 129.44 (C10), 128.80 (C4), 126.25 (C3), 112.18 (C2), 111.87 (C10a), 111.31 (C3a), 110.68 (C8), 110.04 (C9), 107.12 (C6), 102.89 (C5), 47.97 (C1), 39.38 (C11), 37.97 (C20), 33.44 (C16), 33.03 (C14), 32.81 (C15), 32.40 (C18), 30.83 (C19), 27.96 (C12), 27.62 (C13), 26.20 (C17) ppm.

Acknowledgment. We are grateful to the United States-Israel Binational Science Foundation (BSF) and the Natural Sciences and Engineering Research Council (NSERC) of Canada for financial support.

JA040039U